

Magnetotransport and thermopower properties of the quasi-two-dimensional charge-density-wave compounds $(\text{PO}_2)_4(\text{WO}_3)_{2m}$ ($m=4,6$)

C. Hess, C. Schlenker,[†] and J. Dumas

*Laboratoire d'Etudes des Propriétés Electroniques des Solides, CNRS, Boîte Postale 166, 38042 Grenoble Cedex 9, France**

M. Greenblatt and Z. S. Teweldemedhin

Department of Chemistry, Rutgers, The State University of New Jersey, Piscataway, New Jersey 08855-0939

(Received 7 March 1996)

Magnetoresistance, Hall effect, and thermopower have been measured between 4.2 and 300 K on the monophosphate tungsten bronzes $(\text{PO}_2)_4(\text{WO}_3)_{2m}$, with $m=4$ and 6. The Peierls transitions associated with charge-density-wave gap openings appear clearly on all explored properties. In the normal state, both compounds behave as nearly compensated metals, the transport and cyclotron carriers having different signs as a consequence of the complex morphology of the Fermi surface, in agreement with previous band-structure calculations. The anisotropic thermopower found in the charge-density-wave state of the $m=6$ compound gives information on the carrier pockets left by the gap openings along different crystallographic directions. This result is discussed in relation to previous x-ray determination of the nesting wave vectors. A two-band model used to evaluate the sizes of these pockets shows that they are smaller in the $m=6$ than in the $m=4$ phase. This finding is attributed to a stronger low-dimensional character in the $m=6$ material, which leads to better nesting properties of the Fermi surface. [S0163-1829(96)05231-9]

I. INTRODUCTION

The monophosphate tungsten bronzes belong to the large family of the quasi-two-dimensional (2D) inorganic conductors which often show electronic instabilities. Their history goes back to approximately 30 years ago, when the transition-metal-layered dichalcogenides were extensively studied, mostly in relation to their strongly anisotropic anomalous conducting properties.¹ These phenomena were soon attributed to the Peierls instability induced by special properties of the Fermi surface (FS), combined with strong electron-phonon coupling and leading to the so-called charge-density-wave (CDW) state at low temperature.^{2,3} It was shown later that similar properties are found in some quasi-2D molybdenum bronzes and oxides.⁴ More recently, the series of the monophosphate tungsten bronzes $(\text{PO}_2)_4(\text{WO}_3)_{2m}$ (Ref. 5–7) has provided a model system where the low-dimensional character can be modified without changing the band filling. Concurrently, the discovery of superconductivity at high temperature in some copper-based quasi-2D oxides has revived the interest in quasi-2D conducting oxides.⁸

It is now well known that quasi-2D metals can in fact show two types of electronic instabilities, either the Peierls instability⁹ leading to a charge-density wave state,^{6,10} as in some layered transition metal dichalcogenides and in some transition-metal bronzes and oxides,^{4,5} or to superconductivity as in the copper-based high- T_c oxides.⁸ The mechanisms which control the type of instability that actually takes place are not well understood at the moment.

One should also note that the mechanism of the Peierls instability in the quasi-2D conductors is not straightforward, since it is directly related to the so-called nesting properties of the FS.^{6,10} In an ideal 1D metal, the FS, being composed of two parallel planes separated by the vector $2k_F$, is per-

fectly nested and the Peierls instability completely destroys this FS, thus inducing a metal-insulator transition. This is not the case in a 2D metal, where the FS is quasicylindrical and normally shows perfect nesting for a given wave vector only along a line parallel to the cylinder axis. In fact, there is a special case, for a perfect square lattice with one conduction electron per site, where the FS is perfectly nested for the two wave vectors $[110]$ and $[1\bar{1}0]$.¹¹ Real materials do not usually fit into this case.

In this context, it is interesting to study another family of quasi-2D metals, the monophosphate tungsten bronzes, of general formula $(\text{PO}_2)_4(\text{WO}_3)_{2m}$.¹² These materials have been synthesized, and their crystal structure studied for more than ten years.^{13,14} Their lattice is orthorhombic and built with perovskite ReO_3 -type infinite layers of WO_6 octahedra parallel to the ab plane, separated by PO_4 tetrahedra. Since the $5d$ conduction electrons are located in the WO_6 layers, the electronic properties are quasi-2D. The thickness of the ReO_3 blocks, and therefore the c parameter, are increasing with m , while a and b are only weakly dependent on it. The number of conduction electrons per primitive cell is always four, independent of m . On the other hand, the low-dimensional character is expected to change with the thickness of the WO_6 layers. Also, the average number of conduction electrons per W is $2/m$, therefore decreasing with increasing m . The lower carrier density may lead to increased electron-electron interactions due to weaker screening effects.

Band-structure calculations using a tight-binding extended Hückel method in a 2D approximation have been performed for the $m=4$ and 6 compounds. These calculations lead to three bands crossing the Fermi level. The three corresponding sheets of the FS have also been obtained.¹⁵ Nesting properties appear on the resulting FS obtained from the superposition of these sheets. This has been related to the so-called hidden nesting,¹⁶ or hidden one dimensionality, due

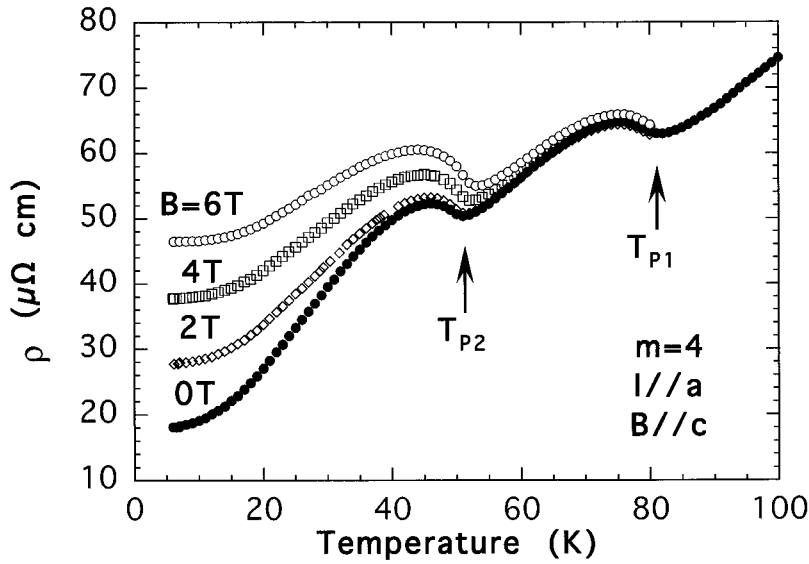


FIG. 1. Resistivity of $P_4W_8O_{32}$ ($m=4$) as a function of temperature for different magnetic fields B . The current is parallel to the a crystallographic axis, and the field B is along c .

to the presence of infinite chains of WO_6 octahedra along the a and $(a \pm b)$ axis. The FS can then be described as being due in a first approximation to the superposition of three quasi-1D FS's. A similar mechanism has been invoked to account for the existence of Peierls instabilities in the 2D molybdenum bronzes and oxides. This type of mechanism therefore underlies the CDW properties of the quasi-2D transition-metal bronzes.

The electrical resistivity of the $m=4$ and 6 members, obtained with current in the ab plane, have been reported in Refs. 17 and 18. Two anomalies in the electrical resistivity, indicating the existence of two electronic instabilities, have been found for $m=4$ at $T_{P1}=80$ K and $T_{P2}=52$ K. Data obtained with current along the c axis indicate that the resistivity is at least a factor 5 higher along this direction in the case $m=6$.¹⁷ X-ray diffuse scattering studies have demonstrated that they correspond to incommensurate CDW with wave vectors components in the ab plane $\mathbf{q}_1=(0.330, 0.295)$ and $\mathbf{q}_2=(0.340, 0)$.^{19–21} In the case of the $m=6$ phase, these two instabilities are found at $T_{P1}=120$ K and $T_{P2}=62$ K [$\mathbf{q}_1=(0.385, 0)$ and $\mathbf{q}_2=(0.310, 0.295)$], therefore at higher temperatures than for $m=4$. A third instability has also been found at low temperature ($T_{P3}=30$ K) by structural studies with a wave vector $\mathbf{q}_3=(0.29, 0.11)$.^{19–21}

The aim of this paper is to compare the transport properties of the $m=4$ and 6 members of the series, both in the normal and CDW states, in order to find out how the Peierls instability and the nature of the CDW state are affected by a change in the low-dimensional character. Therefore, we report detailed studies of the resistivity, magnetoresistivity, Hall effect, and thermopower. Preliminary results of magnetoresistivity and Hall effect have been given previously.¹² They indicate that anomalies appear in both properties at the Peierls temperatures. We now also report thermopower data which show, in the case $m=6$, a strong anisotropy in the ab plane in the CDW state. We also analyze the magnetotransport properties with a two-band model. All results establish that the destruction of the FS is more complete in the $m=6$ compound than in $m=4$. This is consistent with a better Fermi-surface nesting and therefore an increase of the low-dimensional character with increasing m parameter.

II. EXPERIMENT

Single crystals used in these studies have been grown by solid-state reaction¹⁷ or by chemical vapor transport technique.¹⁸ The crystals are in shape of platelets parallel to the ab conducting plane, and are of typical size $1.5 \times 0.5 \times 0.05$ mm³. Electrical contacts were applied by first washing the samples in acetone and in either HF (5%) or NH_3 (28%) at 70 °C for 1 h, then evaporating a silver layer and gluing gold wires (25 μ m) with silver paste onto the contact pads.

The resistivity and thermopower measurements have been performed in a He^4 cryostat over temperatures from 4.2 or 8 K to 300 K, respectively. The resistivity was measured by a standard four-probe technique. Thermopower data were obtained using a slow ac (0.01 Hz) technique similar to the one described in Ref. 22. The ends of the crystal are fixed by two gold foils and glued with silver paste, assuring a good thermal contact to the heating blocks. The latter are used to apply an alternating thermal gradient across the sample (max ± 1 K). The Seebeck voltage and the corresponding temperature difference measured by a Au-Fe thermocouple are collected during three measurement cycles, while the whole setup is kept at a constant temperature. The experiment is entirely computer controlled.

Magnetoresistance and the Hall effect were measured in a He^4 cryostat equipped with a superconducting coil providing magnetic fields up to 6 T. The magnetic field was always perpendicular to the ab plane. The Hall voltage was obtained from the difference of the transverse voltages for the two field orientations.

We will first report results obtained on the compound $m=4$ ($P_4W_8O_{32}$). Figure 1 shows the in-plane resistivity ρ and magnetoresistivity parallel to the a axis as a function of temperature for the $m=4$ compound.^{12,18} Absolute values of ρ are of the order of 20 $\mu\Omega$ cm at 4 K. Two distinct anomalies found as previously at $T_{P1}=80$ K and $T_{P2}=50$ K correspond to the Peierls instabilities and to the formation of two incommensurate charge-density waves.²¹ A giant magnetoresistance is found for magnetic fields perpendicular to the ab layers. Hall-effect data shown as a function of temperature in

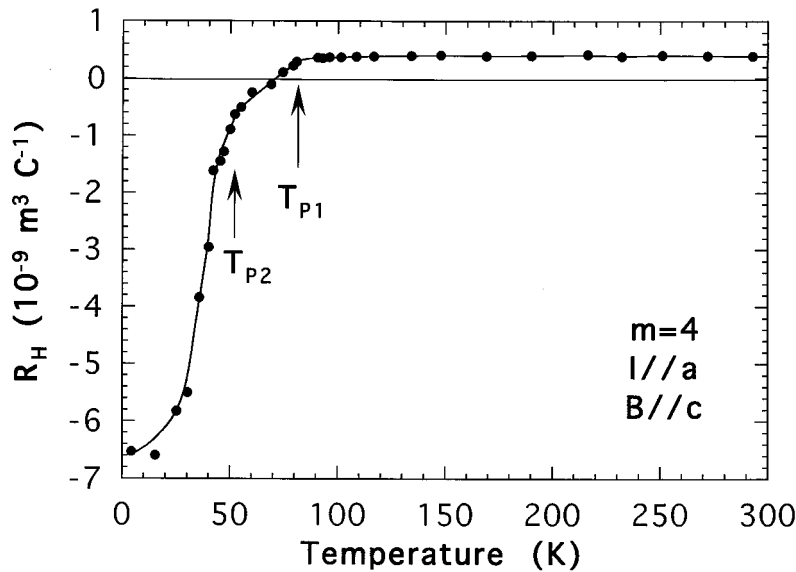


FIG. 2. Hall coefficient as a function of temperature for $m=4$. The current is along a and the field along c .

Fig. 2 are obtained for a current injection along the crystallographic a axis with the magnetic field along c . A constant positive Hall coefficient is found in the high-temperature normal state ($R_H = 0.4 \times 10^{-9} \text{ m}^3 \text{ C}^{-1}$). The Peierls transitions can be detected as kinks in the curve leading to a negative Hall coefficient in the CDW state. Below these transitions, the Hall voltage is found to be linear vs B only in low fields ($B < 0.5$ to 1 T depending on the temperature): in this case the collected R_H data correspond to the low-field limit. The thermoelectric power (TEP) is shown in Fig. 3. The temperature gradient was applied along the a direction. The absolute values of S are in the range 0 – $20 \text{ } \mu\text{V K}^{-1}$. A quasilinear behavior with a negative slope is found in the metallic state. This slope changes at the Peierls temperatures, and a deep minimum can be seen in the temperature range from 20 to 40 K. Since the same behavior has been observed for the $a \pm b$ and b directions, the TEP of $m=4$ is isotropic in the ab plane.

The results of the electrical resistivity and magnetoresis-

tivity vs temperature obtained for the $m=6$ compound are shown in Fig. 4. Two humps in the curves corresponding to Peierls transitions at $T_{P1} = 120$ K and $T_{P2} = 60$ K are clearly observed. There is, however, no evidence of the third instability detected previously by x-ray diffuse scattering at $T_{P3} = 30$ K.¹⁹ The absolute values of resistivity are about several hundred $\mu\Omega \text{ cm}$ at 4 K, and at least one order of magnitude larger than the ones measured for $m=4$.¹⁷ A very large magnetoresistance is found below T_{P2} . These results confirm earlier ones.¹² The Hall coefficient has been measured in the same configuration as for the $m=4$ member (Fig. 5). The high temperature $T > T_{P1}$ regime corresponds to a weakly positive Hall coefficient as for $m=4$ ($R_H = 0.5 \times 10^{-9} \text{ m}^3 \text{ C}^{-1}$). By contrast, it becomes more positive in the Peierls state below T_{P1} and T_{P2} with sharp kinks at the transition temperatures. A weak anomaly around 30 K could be a hint of the third Peierls transition.²³ The thermopower is highly anisotropic in the Peierls state with values in the range -30 to $+40 \text{ } \mu\text{V K}^{-1}$ (Fig. 6). In the high-temperature regime, the

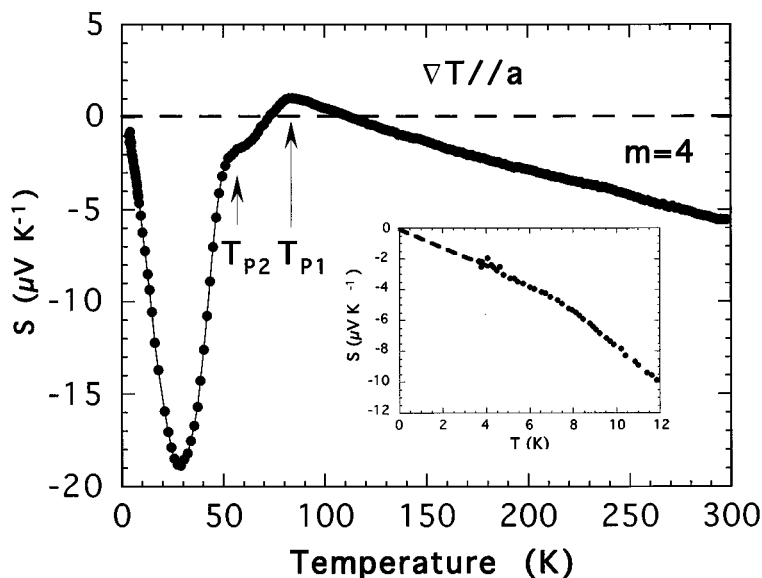


FIG. 3. Thermoelectric power of $m=4$ as a function of temperature. The temperature gradient is along a . The inset shows the low-temperature data. The broken line is a guide to the eye.

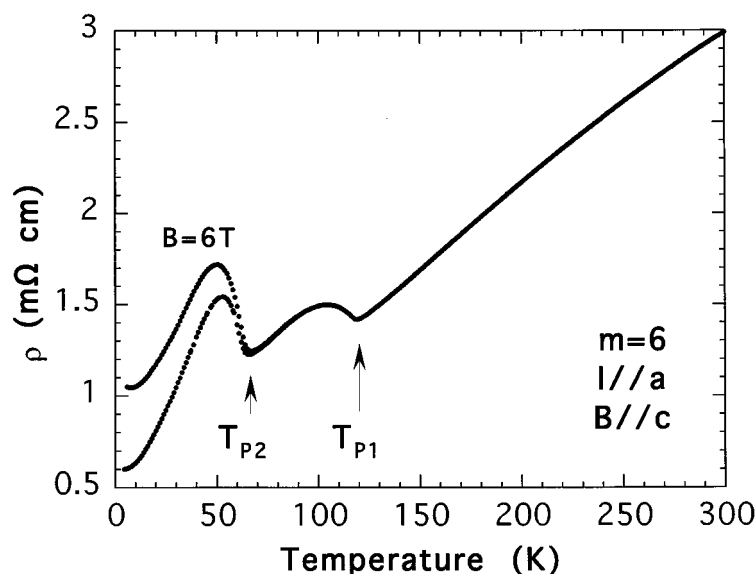


FIG. 4. Resistivity of $P_4W_{12}O_{44}$ ($m=6$) as a function of temperature with magnetic field $B=6$ T (upper curve) and $B=0$ (lower curve). The current is along the a crystallographic axis and the field B along c .

TEP shows a quasi-linear and isotropic behavior along a and b crystallographic directions. The negative slope is a factor 2 smaller than in the case $m=4$. Below T_{P1} the TEP along b becomes more negative, whereas for the a direction the curve flattens out. Below T_{P2} , an increase is observed for both directions. Along a , the TEP shows a broad maximum in the temperature range from 20 to 40 K. The measurement along b , however, reveals an anomaly around $T=30$ K, coinciding with the third Peierls transition.

III. DISCUSSION

We will first discuss the properties of the normal metallic state of both compounds, and in a second part those of the low-temperature CDW states.

A. Normal state

Above the higher Peierls temperature, the monophosphate tungsten bronzes $m=4$ and 6 are expected to behave as normal metals below or close to the Debye temperature, since

this temperature has been found to be roughly 280 K for $m=4$ and 240 K for $m=6$.²⁴ However, one should note that in both compounds the TEP is found to be with a negative slope, while the Hall constant is positive. This finding indicates that both bronzes are nearly compensated metals. Band-structure calculations predict that three bands cross the Fermi level.^{15,25} The highest one is electronlike in all directions, the middle one is expected to be electronlike (or flat) along the a axis and holelike along b , while the opposite behavior is expected for the lowest band in both compounds (Fig. 7). The TEP is found to be electronlike in the normal state, whatever the direction of the temperature gradient is; this may therefore indicate that the highest band is associated with the longer relaxation time, and it primarily determines the transport mass and therefore the sign of the thermopower. On the other hand, the sign of the Hall coefficient is determined by the cyclotron properties and by the electron trajectories along the section of the FS in the ab plane. Our results show that the cyclotron mass is predominantly associated with hole-type carriers. Similar results have been

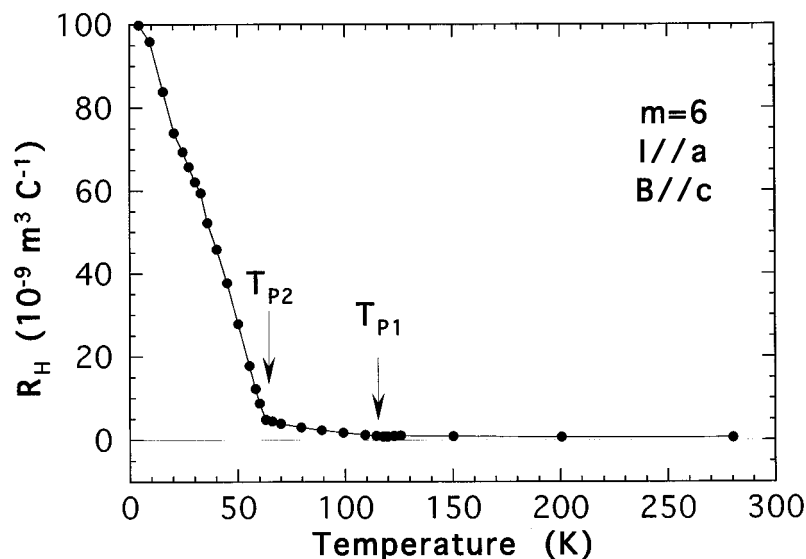


FIG. 5. Hall coefficient as a function of temperature ($m=6$). The current is along a and the field along c .

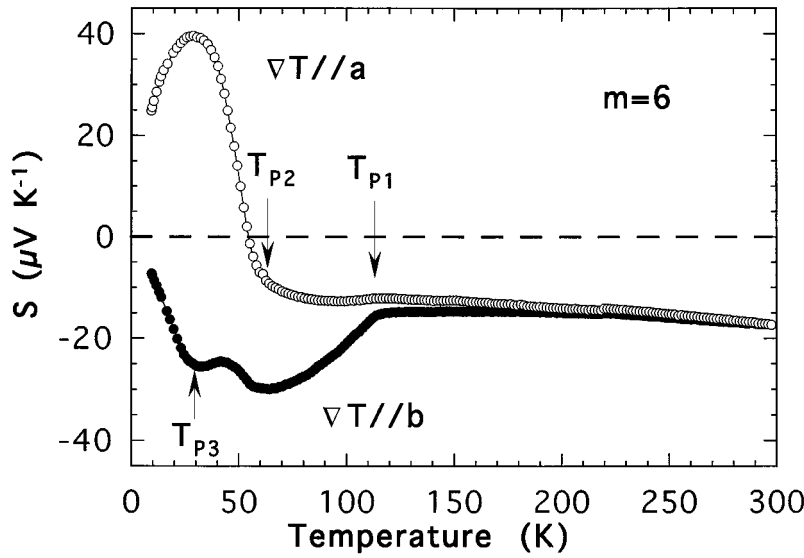


FIG. 6. Thermoelectric power as a function of temperature for $m=6$. Upper curve (open circles): Temperature gradient along the a crystallographic axis. Lower curve (filled circles): temperature gradient along b .

found for the high- T_c superconducting oxides, and attributed to the complex morphology of the FS.²⁶

Although the band structure is rather complicated, it is interesting to compare the carrier concentration n_{chem} evaluated with the chemical formula ($2/m$ per W ion) and the values n_{eff} obtained from the Hall effect with the simple Drude model. One obtains in both cases values of the order of 10^{22} cm^{-3} , smaller as expected for $m=6$ than for $m=4$ ($n_{\text{chem}}=0.7 \times 10^{22}$ and $0.5 \times 10^{22} \text{ cm}^{-3}$ for $m=4$ and 6, respectively, as well as $n_{\text{eff}}=1.6 \times 10^{22}$ and $1.25 \times 10^{22} \text{ cm}^{-3}$). The values of the slope of the TEP at high temperature cannot be accounted for by a simple analysis. One can try to extract values of a Fermi energy ε_F through the classical formula $S = -\pi^2 k^2 T / 2e \varepsilon_F$, assuming a one-band model

with an energy-independent relaxation time. Values of the order of several eV are found. These values are inconsistent with the depth of the highest conduction band involved in the TEP (12 and 55 meV for $m=4$ and 6, respectively) [Fig. 7(a)]. This observation is corroborating evidence that the monophosphate tungsten bronzes are nearly compensated metals in the normal state.

B. Charge-density-wave states

In both compounds, the nesting properties of the FS combined with electron-phonon coupling induce successive Peierls instabilities which partly destroy the FS. One should note that the Peierls temperatures are higher for $m=6$ than for $m=4$, while the normal-state resistivity $\rho_{300 \text{ K}}$ is also approximately one order of magnitude larger in $m=6$. This difference in behavior cannot be accounted for only by the difference in the calculated carrier concentration, which is expected to be much smaller. Therefore, it has to be attributed either to a stronger electron-phonon coupling in $m=6$ compared to $m=4$, or to stronger electron-electron interactions due to a weaker screening.

One may try to extract some information on the CDW FS and carrier concentration using magnetotransport and TEP data. As previously suggested,¹² the giant positive magnetoresistance in the CDW state indicates that the compounds are nearly compensated metals,²⁷ and that the FS includes several electron and hole pockets with high mobilities. In principle, it is possible to analyze the magnetotransport properties by using the so-called two-band model. This analysis is valid for two-band systems if the magnetoresistivity $\Delta\rho/\rho$ and the Hall coefficient follow the field dependences given in Ref 27: $\Delta\rho/\rho$ should vary as B^2 in low fields. It should saturate in high fields, except if the metal is perfectly compensated. R_H should be field independent in the limit of low fields. In our case $\Delta\rho/\rho$ does not saturate in high fields.¹² One may therefore assume a full compensation, and take the electron concentration n to be equal to the hole concentration p . In the rough approximation of only two bands and using the measured values of the conductivity, of R_H and of $\Delta\rho/\rho$, one may evaluate the carrier concentrations and the mobilities μ and ν of the electrons and holes, respectively. The results are

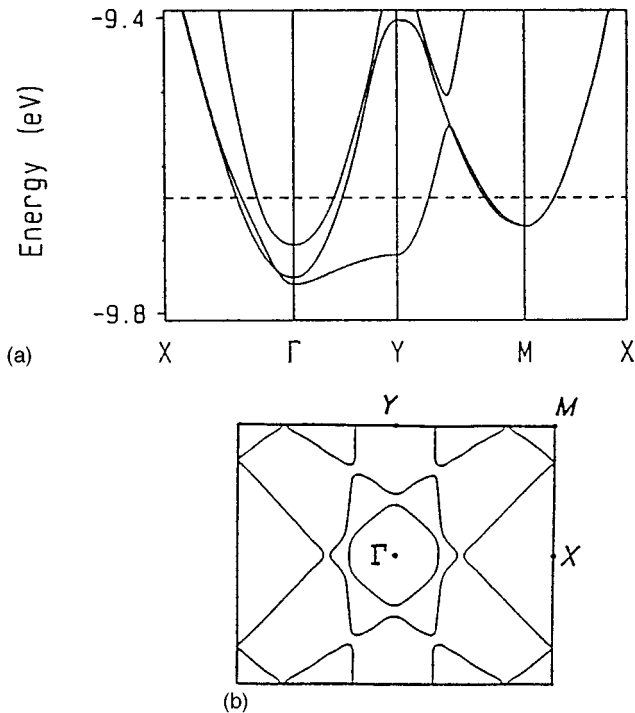


FIG. 7. $\text{P}_4\text{W}_{12}\text{O}_{44}$ ($m=6$): (a) Band structure, (b) Fermi surface (from Ref. 15).

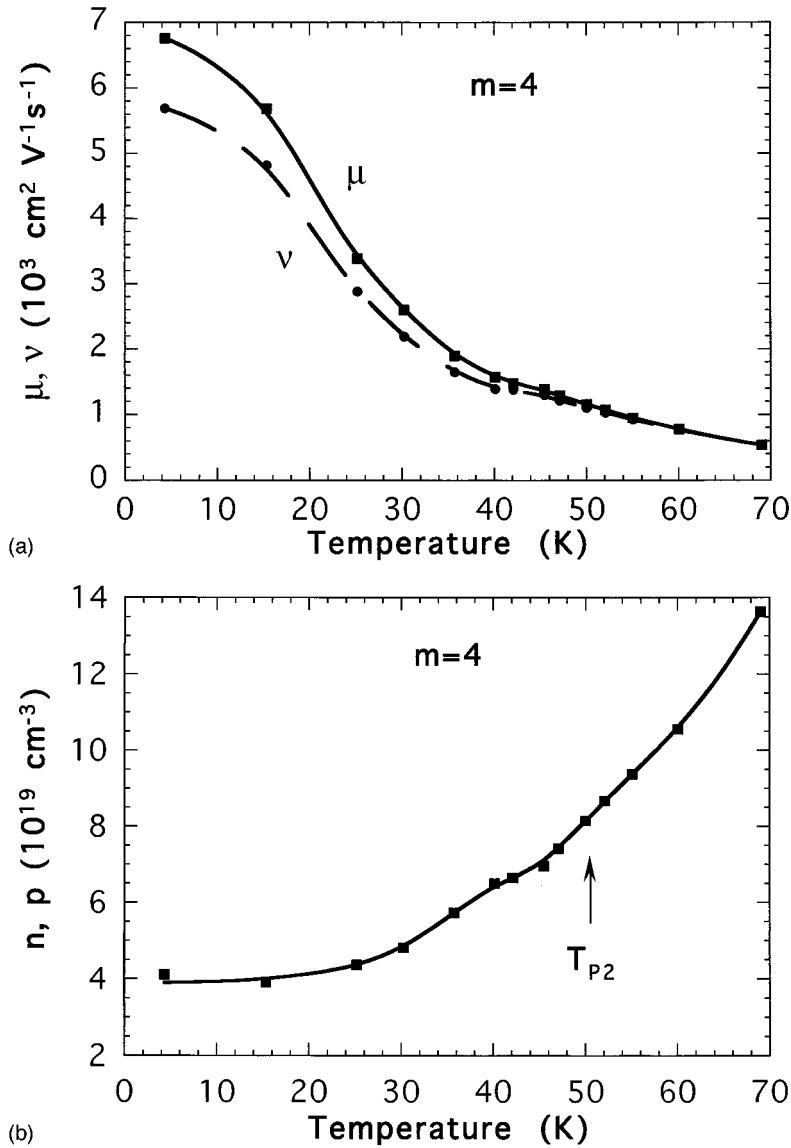


FIG. 8. (a) Mobilities μ of electrons and ν of holes as a function of temperature evaluated with a two-band model assuming perfect compensation ($n=p$) for $\text{P}_4\text{W}_8\text{O}_{32}$ ($m=4$). (b) Carrier densities n and p as a function of temperature obtained with the same model.

shown in Figs. 8 and 9 for $m=4$ and 6. For $m=4$, these parameters can be obtained only below 70 K, when the magnetoresistivity is large enough. The carrier concentrations are found to decrease down to roughly 20 K, therefore to approximately $T_{P2}/2$, when the CDW gap should saturate [Fig. 8(b)]. The value of n and p ($4 \times 10^{19} \text{ cm}^{-3}$ at low temperature) is found to be three orders of magnitude smaller than in the normal state. As expected, the carrier mobilities are found to increase steeply at low temperature, reaching values of the order of several thousands $\text{cm}^2 \text{ V}^{-1} \text{ s}^{-1}$ at 10 K [Fig. 8(a)]. This result was compared to the effective mobility evaluated at room temperature with a simple Drude model ($\mu = R_H/\sigma$), and found to be of the order of $1 \text{ cm}^2 \text{ V}^{-1} \text{ s}^{-1}$. Similar results are found for $m=6$ (Fig. 9). However, in this second case, one obtains a much steeper decrease of n and p below T_{P2} , and low-temperature values one order of magnitude smaller than for $m=4$ [Fig. 9(b)]. Also a weak anomaly is found below 30 K, which might be associated with the third Peierls instability at T_{P3} .

The low-temperature carrier concentrations have to be compared to the results of quantum transport obtained in both compounds.²⁸ The size of the pockets giving rise to

Shubnikov–de Haas oscillations have been found to correspond to an area of 5.4% of the high-temperature two-dimensional Brillouin zone for $m=4$ and only of 1.1% for $m=6$. All these results are therefore consistent, and show clearly that the FS is more completely destroyed in the $m=6$ than in the $m=4$ compound. We propose that this is due to better nesting properties of the FS for larger m in the normal state. This could be related to the increased thickness of the infinite layers of WO_6 , which may result in a weaker transverse coupling if the conduction electrons are confined toward the center of the layers. The quasicylindrical FS would therefore be less warped for larger m , and would show better nesting properties.

The anomalies found at the Peierls temperatures in the curves of the TEP vs T (Figs. 3 and 6) are due to the gap openings which modify the density of states at the Fermi level and the carrier mobility. In the $m=4$ compound, an enhancement of the negative thermopower is found at both transitions, whatever the temperature gradient direction in the ab plane is. This finding shows that electron-type pockets dominate the CDW states, in agreement with Hall-effect data. The peak found at 30 K can be attributed to phonon

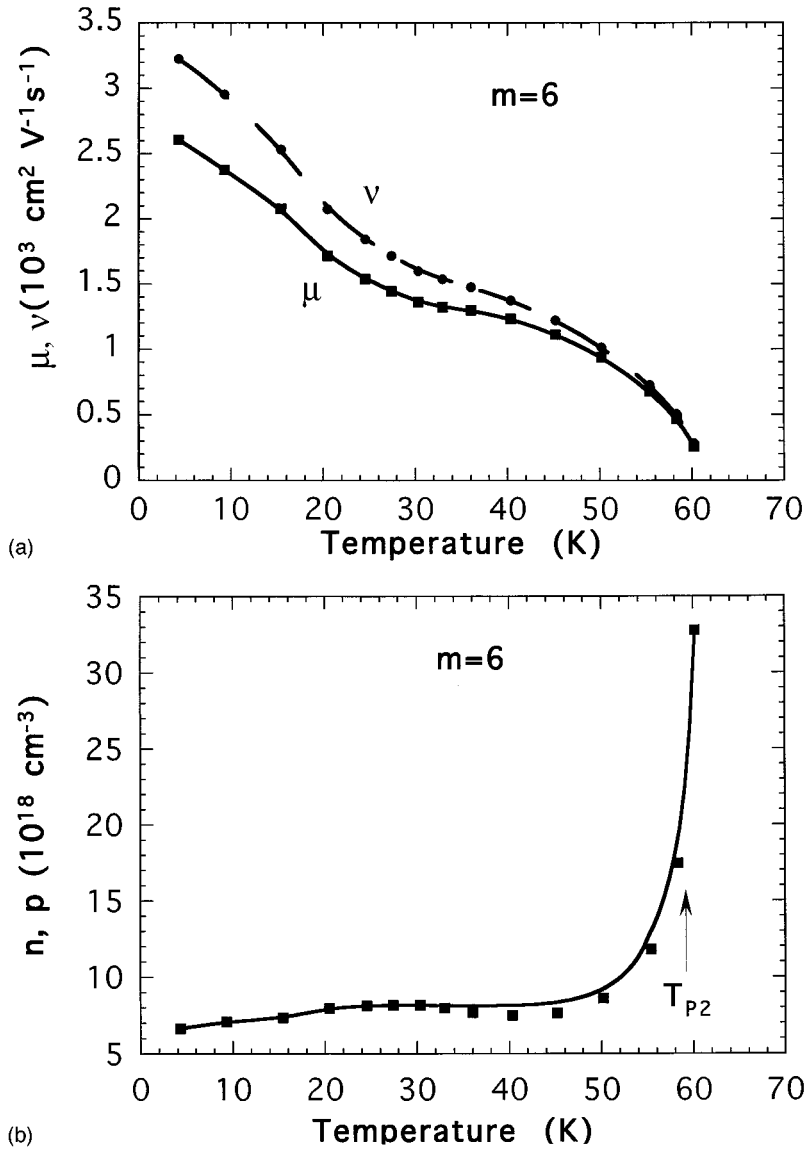


FIG. 9. (a) Mobilities μ of electrons and ν of holes as a function of temperature evaluated with a two-band model assuming perfect compensation ($n=p$) for $\text{P}_4\text{W}_{12}\text{O}_{44}$ ($m=6$). (b) Carrier densities n and p as a function of temperature obtained with the same model.

drag effect,²⁹ since the Debye temperature θ_D has been found to be 280 K,²⁴ and since the maximum of the phonon drag TEP is expected around $\theta_D/10$. However, it is puzzling that below roughly 5 K, the TEP is nearly linear vs temperature (see the inset of Fig. 3), while a T^3 law would be expected in a phonon drag regime at low temperature.

The results obtained for the TEP on $m=6$ differ from the $m=4$ case mainly by the strong anisotropy found in the CDW state. The Seebeck coefficient S is clearly p type when the temperature gradient is along the a axis, and n type along b . This indicates that the CDW pockets induced by the T_{P1} transition are predominantly electrons along b and holes along a . The difference between $m=6$ and 4 must be related to the position of the CDW satellites which are along a^* in the first case and close to $(a^* + b^*)/3$ in the second one.^{19–21} The hole-type behavior along a indicates that the TEP is dominated by carriers left from the Fermi sheet corresponding to the lower band (first Brillouin zone), which have a p -type behavior due to the negative curvature along this direction [Fig. 7(a)]. Below T_{P2} , the TEP indicates that hole-type pockets are induced by this second gap opening. The third instability temperature T_{P3} appears as extrema in the

curve of the TEP vs temperature (Fig. 6). Since phonon drag peaks would be expected in the same temperature range, it is difficult to make a conclusion about the origin of these extrema.

IV. CONCLUSION

The magnetotransport and thermopower data obtained on the $m=4$ and 6 members of the monophosphate tungsten bronzes $(\text{PO}_2)_4(\text{WO}_3)_{2m}$ give information on the Fermi surface both in the high-temperature normal state and in the low-temperature charge-density-wave states. The results obtained in the normal state are consistent with band-structure calculations: both compounds behave as nearly compensated metals due to the combination of three Fermi-surface sheets with different curvatures. Different signs found for the Hall and Seebeck coefficients are due to differences in the transport and cyclotron carriers related to the complex morphology of the FS.

In the CDW state, a strong anisotropy is found for the thermopower of the $m=6$ compound but not for $m=4$. This finding is related to the properties of the high-temperature

FS, and types of carrier pockets expected in the CDW state from the nesting and CDW satellite wave vectors. In the low-temperature CDW state, carrier densities and mobilities have been evaluated from the magnetotransport properties. The results show that the size of the pockets left by the CDW gap openings are smaller in the case of $m=6$ than $m=4$: this is consistent with the higher Peierls temperatures found in $m=6$, and is attributed to a stronger low dimensionality which results in a less warped cylindrical Fermi surface.

Further work is focused on the compounds with higher values of m which show higher Peierls temperatures and also higher electrical resistivities.⁷ The role of the low-dimensional character and of possible electron-electron inter-

actions can be better studied and analyzed in these compounds.

ACKNOWLEDGMENTS

The authors wish to thank E. Canadell, A. Ottolenghi, J. P. Pouget, and M. Whangbo for helpful discussions. Technical help from R. Buder is acknowledged. This work was partially supported by the programme Human Capital and Mobility of the European Union under Contract No. ERB-CHRXCT940616. C.H. is grateful for support from the Land Baden-Württemberg, Germany.

* Associated to Université Joseph Fourier, Grenoble, France.

† Electronic address: schlenke@lepes.polycnrs-gre.fr

¹ J. A. Wilson and A. D. Yoffe, *Adv. Phys.* **18**, 193 (1969).

² J. A. Wilson, F. J. Di Salvo, and S. Mahajan, *Adv. Phys.* **24**, 117 (1975).

³ R. Friend and A. D. Yoffe, *Adv. Phys.* **36**, 1 (1987).

⁴ *Low-Dimensional Properties of Molybdenum Bronzes and Oxides*, edited by C. Schlenker (Kluwer, Dordrecht, 1989).

⁵ *Oxide Bronzes*, edited by M. Greenblatt [*Int. J. Mod. Phys. B* **7**, 4045 (1993)].

⁶ *Physics and Chemistry of Low-Dimensional Inorganic Conductors*, Vol. 354 of *NATO Advanced Study Institute, Series B: Physics*, edited by C. Schlenker, J. Dumas, M. Greenblatt, and S. van Smaalen (Plenum, New York, 1996).

⁷ C. Schlenker, C. Le Touze, C. Hess, A. Rötger, J. Dumas, J. Marcus, M. Greenblatt, Z. S. Teweldemedhin, A. Ottolenghi, P. Foury, and J. P. Pouget, *Synth. Met.* **70**, 1263 (1995).

⁸ See, for example, *Proceedings of the International Conference on Materials and Mechanisms of Superconductivity—High Temperature Superconductors IV*, edited by P. Wynder [*Physica C* **235-240** (1994)].

⁹ R. Peierls, *Quantum Theory of Solids* (Oxford University Press, Oxford, 1955), p. 108.

¹⁰ *Density Waves in Solids*, edited by G. Gruner (Addison-Wesley, Reading, MA, 1994).

¹¹ S. Tang and J. E. Hirsch, *Phys. Rev. B* **37**, 9546 (1988).

¹² A. Rötger *et al.*, *Europhys. Lett.* **25**, 23 (1994); C. Schlenker, in *Physics and Chemistry of Low-Dimensional Inorganic Conductors* (Ref. 6).

¹³ B. Domengès, F. Studer, and B. Raveau, *Mater. Res. Bull.* **18**, 669 (1983).

¹⁴ P. Labbé, M. Goreaud, and B. Raveau, *J. Solid State Chem.* **61**,

234 (1986).

¹⁵ E. Canadell and M. Whangbo, *Phys. Rev. B* **43**, 1894 (1990); *Chem. Rev.* **91**, 965 (1991); and in *Oxide Bronzes* (Ref. 5), p. 4005.

¹⁶ M. H. Whangbo, E. Canadell, P. Foury, and J. P. Pouget, *Science* **252**, 96 (1991).

¹⁷ E. Wang, M. Greenblatt, I. E. Rachidi, E. Canadell, M. H. Whangbo, and S. Vadlamannati, *Phys. Rev. B* **39**, 12 969 (1989).

¹⁸ Z. S. Teweldemedhin, K. V. Ramanujachary, and M. Greenblatt, *Phys. Rev. B* **46**, 7897 (1992).

¹⁹ P. Foury, J. P. Pouget, E. Wang, and M. Greenblatt, *Europhys. Lett.* **16**, 485 (1991). Only the indices h and k of the CDW wave vectors have been measured in this work.

²⁰ P. Foury, J. P. Pouget, Z. S. Teweldemedhin, E. Wang, M. Greenblatt, and D. Groult, *J. Phys. (France) IV* **3**, C2-133 (1993).

²¹ P. Foury and J. P. Pouget, in *Oxide Bronzes* (Ref. 5), p. 3973.

²² P. M. Chaikin and J. F. Kwak, *Rev. Sci. Instrum.* **46**, 218 (1975).

²³ In Refs. 12 and 24, the Hall-effect data of the $m=6$ compound was given with a sign error in Fig. 4(b) of Ref. 12 and Fig. 2(d) of Ref. 24.

²⁴ J. Lehmann, C. Schlenker, C. Le Touze, A. Rötger, J. Dumas, J. Marcus, Z. Teweldemedhin, and M. Greenblatt, *J. Phys. (France) IV*, **3**, C2-243 (1993).

²⁵ I. E. I. Rachidi, Ph.D. thesis, de l'Université Paris-Sud, 1989.

²⁶ Y. Kubo, *Phys. Rev. B* **59**, 3181 (1994).

²⁷ A. B. Pippard, *Magnetoresistance in Metals* (Cambridge University Press, Cambridge, 1989).

²⁸ C. Le Touze, G. Bonfait, C. Schlenker, J. Dumas, M. Almeida, M. Greenblatt, and Z. S. Teweldemedhin, *J. Phys. (France) I* **5**, 437 (1995).

²⁹ R. D. Barnard, *Thermoelectricity in Metals and Alloys* (Taylor & Francis, London, 1972).